Rapid Deposition of Triangular Silver Nanoplates on Planar Surfaces: Application to Metal-Enhanced Fluorescence

Kadir Aslan,[†] Joseph R. Lakowicz,[‡] and Chris D. Geddes*[,†,‡]

Institute of Fluorescence, Laboratory for Advanced Medical Plasmonics, Medical Biotechnology Center, University of Maryland Biotechnology Institute, 725 West Lombard Street, Baltimore, Maryland 21201, and Center for Fluorescence Spectroscopy, Department of Biochemistry and Molecular Biology, Medical Biotechnology Center, University of Maryland School of Medicine, 725 West Lombard Street, Baltimore, Maryland 21201.

Received: December 18, 2004; In Final Form: February 8, 2005

A simple and rapid wet-chemical technique for the deposition of silver triangles on conventional glass substrates, which alleviates the need for lithography, has been developed. The technique is based on the seed-mediated cetyltrimethylammonium-bromide-directed growth of silver triangles on glass surfaces, where smaller spherical silver seeds that were attached to the surface were subsequently converted and grown into silver triangles in the presence of a cationic surfactant and silver ions. The size of the silver triangles was controlled by sequential immersion of silver seed-coated glass substrates into a growth solution and by the duration time of immersion. Atomic force microscopy studies revealed that the size of the silver triangles ranged between 100 and 500 nm. Interestingly, these new surfaces are a significant improvement over traditional silver island films for applications in metal-enhanced fluorescence. A routine 16-fold enhancement in emission intensity was typically observed, for protein-immobilized indocyanine green, with a relatively very low loading density of silver triangles on the glass surface.

1. Introduction

Solution-based preparation of anisotropic metal nanoparticles has been the subject of many scientific reports in recent years in consideration for applications in nanotechnology.[1−19] Examples of such preparation techniques can be found in the literature for silver nanorods,[2−6] silver triangular nanoplates,[7,8] triangles,[9−13] silver nanowires,[14] and gold nanorods.[15−19] These methods are based on surfactant-based seed-mediated growth,[2,7,8,15−19] thermal growth,[9−11] and photoreduction of metal nanoparticles in solution.[12]

In contrast, the assembly of anisotropic metal nanoparticles on planar surfaces still requires more sophisticated methods such as lithography. One of the more notable examples is "nanosphere lithography" (NSL) developed by Van Duyne and co-workers.[20,21] In this regard, it is informative to clarify the differences between the method presented here and NSL. In NSL, a planar surface (glass or mica) is immersed in a suspension of polystyrene (PS) nanospheres where PS nanospheres self-assemble in a hexagonal close-packed array. The planar surface is then mounted in a vacuum chamber, and silver is deposited as a continuous film on top of the planar surface through a mask created by the close-packed polystyrene particles. The polystyrene particles are removed, leaving the truncated silver tetrahedral nanostructures on the surface. The size of the silver nanostructures and their spacing can be changed by changing the size of PS nanospheres that are used as the physical mask and by varying the amount of deposited metal.[20,21] Although NSL is a very reliable technique to produce well-defined anisotropic silver nanoparticles on solid substrates, it is an expensive and somewhat tedious technology. Thus, there is still a need for much easier and more affordable techniques for the deposition of anisotropic metal structures on planar surfaces.

Recently, Aslan et al.[22] reported the growth of silver nanorods directly on glass using a method based on the solution-seeded nanorod synthesis scheme.[19] This technique was introduced as a first step toward removing the need for wet-chemical lithographic processes. Other examples include the deposition of gold nanorods on mica and conventional glass substrates by Taub et al.[23] and Wei et al.,[24] respectively.

In this work, the deposition of silver triangles on conventional glass substrates, analogous to the wet-chemical method that was applied for the growth of silver nanorods by Aslan et al.[22] on glass substrates is reported. This new approach enables one to control the size/loading density of the silver triangles on the glass substrates by controlling simple experimental parameters such as immersion time, concentration, temperature, and the surfactant. Although, the triangular silver nanostructures are deposited in a random fashion on the glass substrate, these new advances are directed at fabricating new cheap and relatively quickly silvered surfaces for applications in metal-enhanced fluorescence, a technology that has been receiving much attention in the past few years.[26−29]

Over the past several years, the laboratories at the University of Maryland at Baltimore and the University of Maryland Biotechnology Institute have shown the favorable effects that can be obtained for fluorophores in close proximity to metallic surfaces, such as enhanced quantum yields, increased excitation rates (local field enhancement), and an increased fluorophore photostability.[26−29] These experimental platforms have widely utilized both silver island films (SiFs)[29] and silver colloid films[29] and typically resulted between 5- and 30-fold fluorescence

* Author to whom correspondence should be addressed. E-mail: geddes@umbi.umd.edu.
[†] University of Maryland Biotechnology Institute.
[‡] University of Maryland School of Medicine.

10.1021/jp044235z CCC: $30.25
Published on Web 03/15/2005

intensity enhancements with an average optical density of 0.4.[29] However, silver fractal-like surfaces, which were grown by passing a current between silver electrodes in deionized water,[29] have produced spatially localized enhancements of several 1000-fold, which until that time were only predicted by theory.[26] Deposition of rodlike structures on planar surfaces that possess similar characteristics to the fractals with regard to shape and size, but use simple chemistries and no electric currents in their preparation, was reported recently.[22] Similar to nanorods,[22] the triangles deposited on a glass surface in this work are not ordered but are in fact somewhat irregular, producing typical enhancements of indocyanine green fluorescence of ~16-fold, with a relatively very low silver loading density (optical density ≈ 0.08). With the use of metal-enhanced-fluorescence-based phenomena emerging into clinical assays and other aspects of nanotechnology[29], these novel and quickly prepared surfaces could find a common place in routine applications of MEF and replace the more traditional silver-island-film-based MEF platforms. [29]

2. Materials and Methods

2.1. Materials. Silver nitrate (99.9%), sodium citrate (99%), L-ascorbic acid (99%), sodium borohydride (98%), 3-(aminopropyl)triethoxysilane (APS), sodium hydroxide (99.996%), and cetyltrimethylammonium bromide (CTAB, 99%) were obtained from Sigma-Aldrich. All chemicals were used as received. Premium quality glass slides were purchased from Fisher Scientific (75 mm × 25 mm).

2.2. Methods. *2.2.1. Silanization of Glass Substrates.* Glass slides were cleaned with "piranha solution" for at least 2 h (3:7 30% hydrogen peroxide/concentrated sulfuric acid; CAUTION! *Piranha solution reacts violently with most organic materials and should be handled with extreme care*). Then, the glass substrates were rinsed extensively with deionized water and dried in a stream of dry nitrogen prior to use. The cleaned slides were silanized by immersing them in a 2% ethanolic solution of APS for 2 h. Then, the APS-coated glass slides were rinsed in ethanol and then water and sonicated in ethanol for 30 s. Finally, the APS-coated slides were rinsed with water and dried in a stream of nitrogen gas. The silanization of the glass substrates is essential for immobilizing silver.[22,25]

2.2.2. Deposition of Silver Triangles onto Glass Substrates. APS-coated glass slides were immersed in the silver seed (4 nm as reported by Jana et al.[2]) solution for ~30 min, rinsed with deionized water, and then dried in a stream of nitrogen gas. The silver-seed-coated glass slides were then immersed in 40 mL of 0.80 M CTAB solution for 1−3 min. A 1 mL aliquot of 10 mM $AgNO_3$ and 2 mL of ascorbic acid were then added. A 0.4 mL aliquot of 1 M NaOH was immediately added, and the solution was mixed gently to accelerate the growth process. The silver triangles were formed on the glass slides within 5 min, evident by the color change (clear to orange) on the glass slide and also in the solution. To increase the loading (surface optical density) of silver triangles on the surface, the silver-triangle-coated glass substrates were immersed in CTAB again, similar amounts of $AgNO_3$, ascorbic acid, and NaOH being added as in the first step. This process can be repeated until the desired loading of the silver triangles onto the glass slides is achieved (Figure 1).

All absorption measurements were performed using a HP 8453 UV−vis spectrophotometer. Atomic force microscopy (AFM) images were collected using an atomic force microscope (TMX 2100 Explorer SPM, Veeco), equipped with an AFM dry scanner (the scanning area was 100 mm × 100 mm).

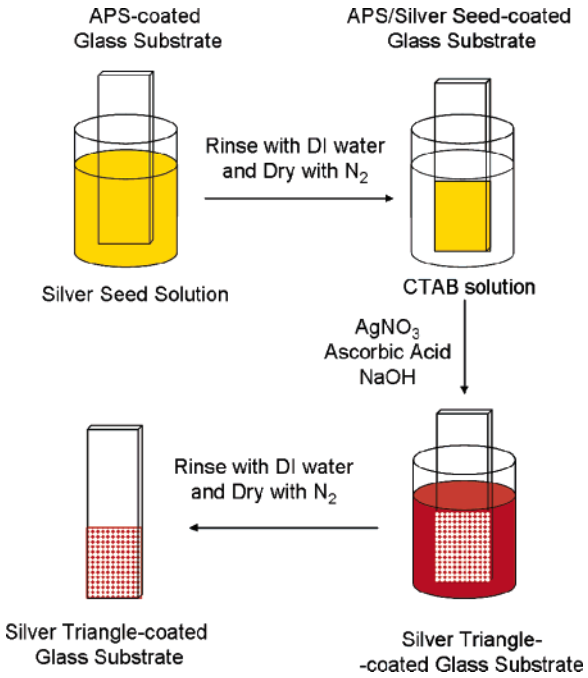

Figure 1. Deposition of silver triangles onto glass substrates.

Surfaces were imaged in air, in a tapping mode of operation, using scanning force microscopy (SFM) noncontact mode cantilevers (Veeco). Samples were freshly prepared prior to imaging. The AFM scanner was calibrated using a standard calibration grid as well as by using gold nanoparticles, 100 nm in diameter from Ted Pella. Images were analyzed using SPMLab software.

2.2.3. Coating of Fluorophore−Protein onto Silver Triangle Surfaces. In this work, the long-wavelength dye indocyanine green (ICG), which is widely used in a variety of in vivo medical applications, is utilized.[34] ICG is nontoxic and is approved by the U. S. Food and Drug Administration for use in humans, typically by injection. ICG displays a low quantum yield in solution, ~ 0.016, [35] making it a good candidate for metal-enhanced fluorescence (MEF), since low quantum yield fluorophores result in greater enhancements,[26] i.e., enhancement = $1/Q_0$, where Q_0 is the quantum yield in the absence of silver. Binding the ICG−human serum albumin (HSA) (ICG is noncovalently bound to HSA) to the silver-triangle-deposited glass slides was accomplished by soaking in a 30 μM ICG, 60 μM HSA solution for 2 h, followed by rinsing with water to remove the unbound material. Both the glass (control sample) and silver-triangle-deposited surfaces were equally coated with the labeled HSA, which is known to passively absorb to noble metal surfaces and form a ~4 nm thick protein monolayer, allowing one to study the fluorescence spectral properties of noncovalent ICG−HSA complexes in the absence and presence of the silver triangles. This experimental format has been adopted for two main reasons, the first being that the protein coverage with HSA is known to bind to silvered surfaces and indeed forms a monolayer[31] and the second being that the dimensions of the protein are such that the protein allows for a mean separation of the silver and the fluorophore, MEF being a through space phenomenon, as demonstrated by the late T. Cotton.[36] In contrast, surface-enhanced Raman scattering (SERS) is known to be a consequence of contact between the species of interest (fluorophore) and the silvered surface.[36]

By equally coating a glass microscope slide with ICG−HSA, the enhancement factor (benefit) obtained from using the silver was determined, i.e., intensity on silver/intensity on glass, given

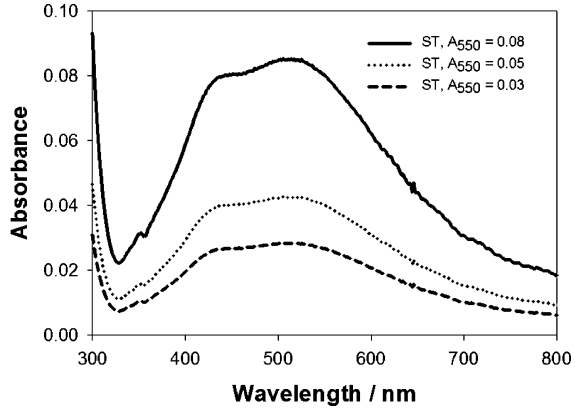

Figure 2. Absorption spectra of silver triangles deposited on glass substrates.

that both surfaces are known to have an approximately equal monolayer coverage by passive absorption.[31] The experimental setup used to observe the emission from both the silvered and the *unsilvered* slides has been reported by the authors previously.[29,30]

3. Results and Disccussion

As briefly mentioned in the Introduction, the aims of this work were twofold, first, to develop a rapid deposition method for silver triangles and second, to investigate their potential use in MEF as an alternative surface to SiFs. The silver triangles were grown on glass substrates by immersing a glass substrate coated with spherical silver nanoparticles (silver seeds) into a solution of CTAB, silver nitrate, and ascorbic acid as explained in the Experimental Section. The characterization of the silver triangles was done by optical density measurements and atomic force microscopy (AFM). Silver triangles grown on glass substrates have two distinct surface plasmon peaks: 440 and 550 nm (Figure 2). The surface plasmon peak at 440 nm is the transverse plasmon peak, and the peak at 550 nm is the longitudinal plasmon peak.[12] The absorption at these wavelengths was increased as the loading density as well as the size of the silver triangles were increased, with no apparent shift in absorption maximum. This suggests that the triangles grow equilaterally. Similar observations were also made by Maillard et al.[12] for triangles with different sizes grown in solution by photoreduction of silver ions by citrate.

Figure 3 shows the AFM image of the silver triangles that are grown on APS-coated glass slides with the highest loading density (A_{550} = 0.08). The loading density of silver triangles was controlled by the time that the glass slides were kept in the CTAB solution (in this case, 3 min) after the silver ions/ascorbic acid and NaOH (used for speeding up the reactions) were added. A graphical analysis of the data shown in Figure 3 reveals that all the silver particles were grown substantially and converted into triangular (80%) and rodlike (20%) particles. The silver triangles were agglomerated, and their size varied between 100 and 500 nm (height from the AFM image). Some silver nanorods were also present in the similar size range with an aspect ratio (length/height) of less than 2.

It was found that keeping the glass substrates coated with silver seeds in CTAB solution for longer than 3 min resulted in conversion of all the silver particles into rodlike structures. The experimental evidence for this observation was provided by Aslan et al.,[22] where the immersion of glass substrates in CTAB solution between 5 and 10 min yielded rodlike structures. It is hypothesized that the triangular silver particles are formed on the glass surface (also in solution) as transient structures during the conversion of silver spheres into silver nanorods and during the conversion of silver nanorods into silver spheres. The evidence for the latter is given in Figure 4. Figure 4 shows the absorption spectra of silver nanorods in solution before, during, and after continuous heating at 40 °C for 48 h. The continuous heating of CTAB-coated silver nanorods in solution results in conversion of the nanorod shapes into triangles and finally into spheres. During heating of the silver nanorods in solution, the color of the solution changed from green to orange and then to

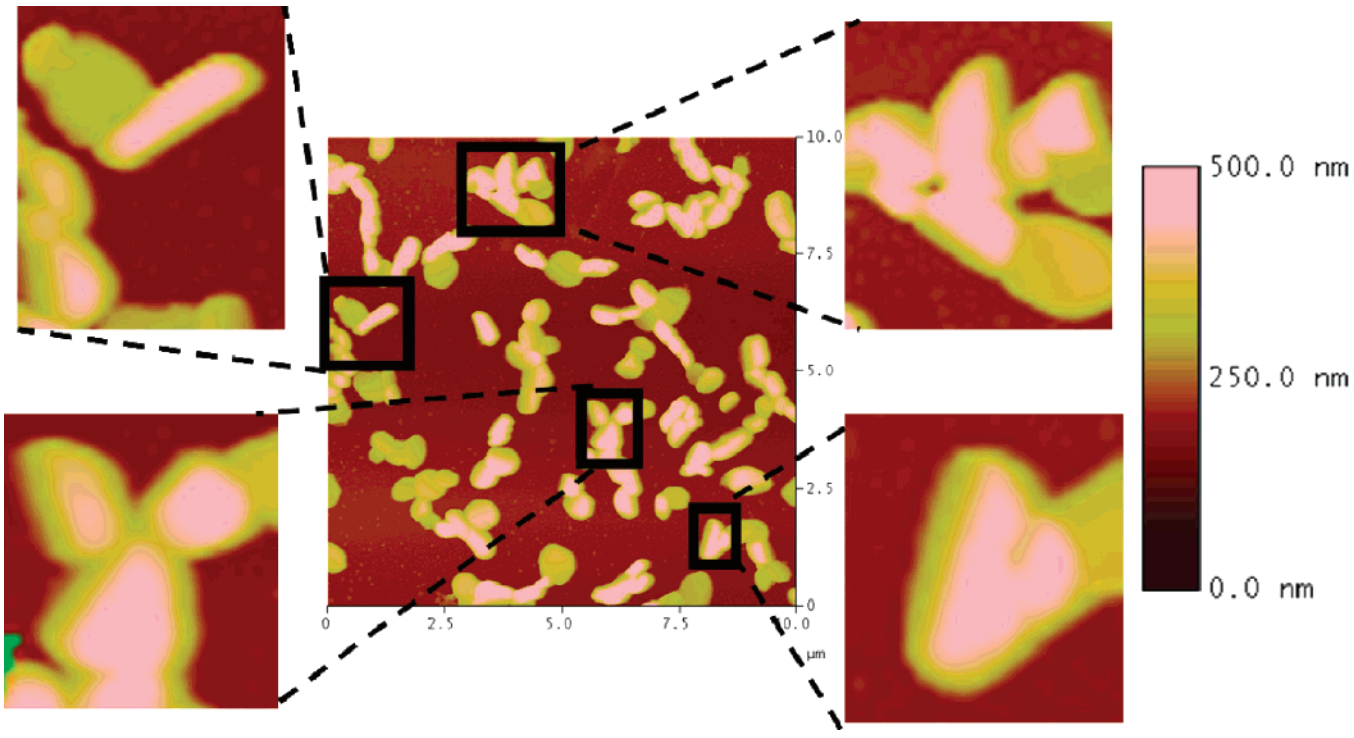

Figure 3. AFM images of silver triangles (80%) and silver nanorods (20%) on glass substrates.

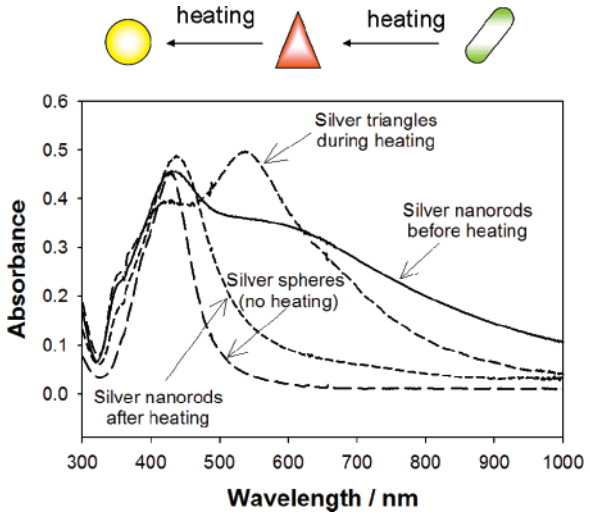

Figure 4. Absorption spectra of silver spheres and silver nanorods before, during, and after heating at 40 °C in solution.

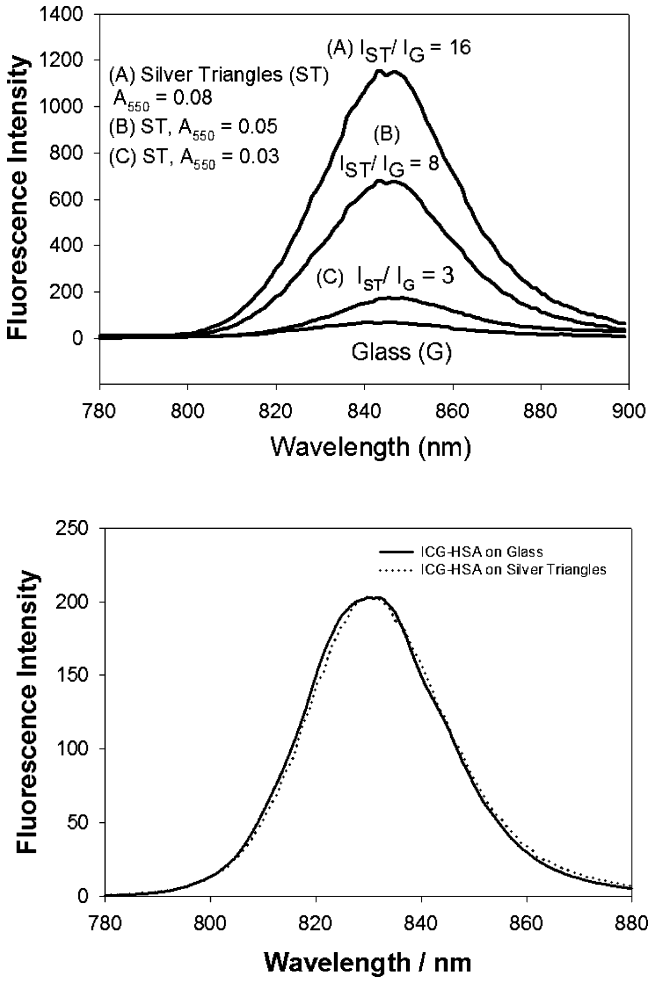

Figure 5. (Top panel) Fluorescence emission intensity of ICG−HSA on silver triangles with different loading densities. The emission intensity of ICG-HSA is 75. (Bottom panel) Normalized emission intensities of ICG-HSA and glass and on silver triangles ($A_{550} = 0.03$), which shows identical spectral behavior.

yellow. Analogous to these observations, the color of the solution and the color of the silver particles deposited on the glass surface changed from clear to yellow and then to orange in 3 min. Longer immersion times (5−10 min) resulted in a solution with a green color. It is well-known that the color of the silver nanoparticle solution depends on the size and shape

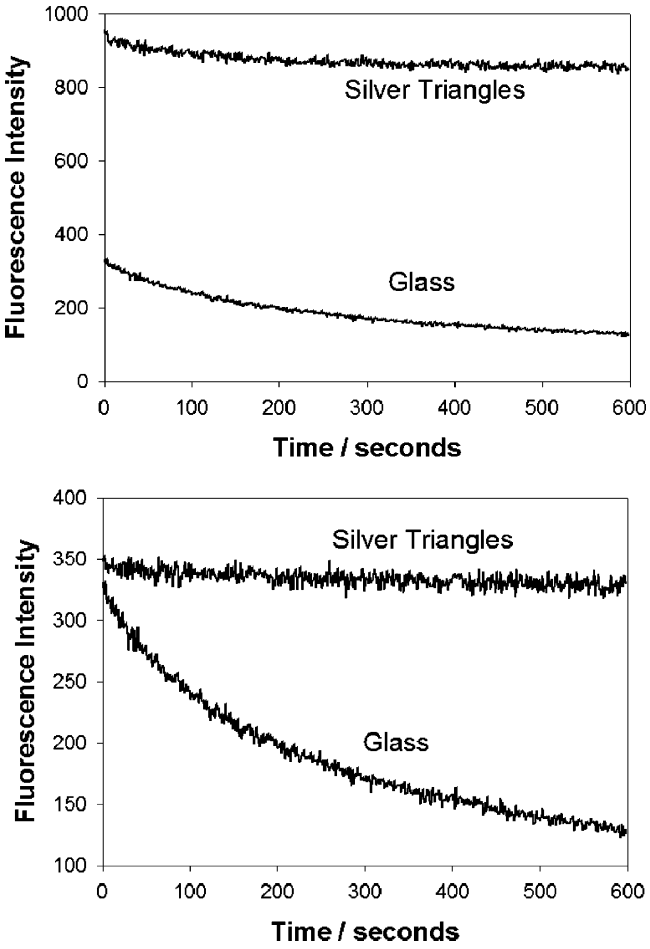

Figure 6. Photostability of ICG−HSA on silver triangles: (top panel) raw data; (bottom panel) normalized data.

of the silver nanoparticles due to their ability to absorb/scatter light and the size and shape of the silver nanoparticles can be controlled by heat.[7,8] While the change in the shape of the silver nanoparticles in Figure 4 is in reverse order (nanorods to spheres), the data provide clear evidence for the order of change with respect to the shape of the silver nanoparticles during the CTAB-assisted conversion process.

The application of these new surfaces, which can be prepared in several minutes, was for MEF, where the close proximity of silver nanostructures can alter the intrinsic radiative decay rate of fluorophores, producing enhanced signal intensities and an increased fluorophore photostability. Several reviews have been reported for this new spectroscopic technology.[26−27]

To test the usefulness of the silver-triangle-coated glass substrates with regard to MEF, the substrates were subsequently coated with ICG−HSA as described in section 2.2.3 and shown in Figure 5. For a low loading density of the triangles on the surface ($A_{550} = 0.03$), a typical fluorescence enhancement of 3 can be obtained relative to the glass surface. However, for higher loadings ($A_{550} = 0.08$), reproducible enhancements of ∼16-fold can be achieved, Figure 5, top panel. Figure 5, bottom panel, also shows that the spectral characteristics of ICG are preserved, as also previously observed with silver island films.[31] In these geometries, enhancements are in the range of 6−20 for ICG but much higher silver optical densities ($A_{420} = 0.4$).[31]

Previous reports have shown that the lifetimes of fluorophores in close proximity to silver nanostructures decrease significantly and the fluorophores become more photostable due to the fact that there is less excited-state time for any photochemical processes to occur.[29−33] In this regard, the photostability of

ICG−HSA when bound to glass and silver triangles was studied. The intensity of ICG−HSA emission was recorded with continuous excitation illumination at 760 nm. When excited with the same incident power, the fluorescence intensities, when considered on the same intensity scale, decreased more rapidly on the glass (Figure 6, top panel) with a greater total photon flux observed from the silvered surface. Alternatively, one can consider the photostability of ICG when the incident laser power is adjusted to result in the same initial emission intensities on silver and on glass. In this case (Figure 6, bottom panel), photobleaching is slower on the silver surfaces. The fact that the photobleaching is not accelerated for ICG and silver indicates that the increased intensities on silver are not due to an increased rate of excitation but indeed are due to a modification of the radiative decay rate of the fluorophore. In this regard, it is worth additionally noting that the fluorescence enhancements observed in Figure 5 and the ratio of integrated areas under the curve in Figure 6, top panel, are not due to reflected photons from the silver but are in fact due to a modification of the intrinsic emissive rate of the fluorophore.[29] This effect is known to be due to the coupling of the surface plasmons on the metallic silver with the oscillating dipole of the fluorophore. [26, 29]

4. Conclusions

The deposition of triangular silver nanostructures on conventional glass substrates, using a CTAB-mediated growth method has been demonstrated. AFM studies have revealed that the silver triangles were irregular-shaped and varied between 100 and 500 nm in size. Proof-of-principle for the application of silver-triangle-deposited surfaces for metal-enhanced fluorescence is shown, where up to a 16-fold enhancement in the intensity of ICG, when compared to *unsilvered* surfaces, coupled with the increased photostability of ICG, were observed. At present, the theory for the metal-enhanced fluorescence phenomenon is relatively poorly understood,[37] as compared to that for fluorescence enhancements produced by the "field enhancement effect", but recent interpretations in terms of a radiating plasmon model[37,38] may allow for a more quantitative description soon. In any case, this new triangle preparation procedure is likely to become common place for applications of MEF, because it is both a much quicker and cheaper alternative as compared to surfaces fabricated by traditional nanolithographic techniques.

Acknowledgment. This work was supported by the National Institutes of Health (GM070929). Partial salary support to C.D.G. and J.R.L. from the University of Maryland Biotechnology Institute is also acknowledged.

Acronyms

AFM = atomic force microscopy
APS = 3-(aminopropyl)triethoxysilane
CTAB = cetyltrimethylammonium bromide
HSA = human serum albumin
ICG = indocyanine green
MEF = metal-enhanced fluorescence
RDE = radiative decay engineering
SEF = surface-enhanced fluorescence
SERS = surface-enhanced Raman scattering
SiFs = silver island films
TEM = transmission electron microscopy

References and Notes

(1) Xia, Y.; Yang, P.; Sun, Y.; Wu, Y.; Mayers, B.; Gates, B.; Yin, Y.; Kim, F.; Yan, H. *Adv. Mater.* **2003**, *15*, 353.
(2) Jana, N. R.; Gearheart, L.; Murphy, C. J. *Chem. Commun.* **2001**, *7*, 617.
(3) Zhu, J. J.; Liao, X. H.; Zhao, X. N. *Mater Lett.* **2001**, *49*, 91.
(4) Xiong, Y. J.; Xie, Y.; Du, G. O. *Chem Lett.* **2002**, *1*, 98.
(5) Hu, J. Q.; Chen, Q.; Xie, Z. X. *Adv. Funct. Mater.* **2004**, *14*, 183.
(6) Chen, D. L.; Gao, L. *J. Cryst. Growth* **2004**, *264*, 216−222.
(7) Chen, S. H.; Fan, Z. Y.; Carroll, D. L. *J. Phys. Chem. B* **2002**, *106*, 10777.
(8) Chen, S. H.; Carroll, D. L. *Nano Lett.* **2002**, *2*, 1003.
(9) Sun, Y.; Mayers, B.; Xia, Y. *Nano Lett.* **2003**, *3*, 675.
(10) Jin, R.; Cao, C.; Hao, E.;. Metraux, G. S.; Schatz, G. C.; Mirkin, C. A. *Nature* **2003**, *42*, 487.
(11) Callegari, A.; Tonti, D.; Chergi, M. P. *Nano Lett.* **2003**, *3*, 1565.
(12) Maillard, M.; Huang, P.; Brus, L. *Nano Lett.* **2003**, *3*, 1611.
(13) Junior, A. M.; de Oliveria, H. P.l; Gehlen, M. H. *Photochem. Photobiol. Sci.* **2003**, *2*, 921.
(14) Caswell, K. K.; Bender, C. M.; Murphy, C. J. *Nano Lett.* **2003**, *3*, 677.
(15) Jana, N. R.; Gearheart, L.; Murphy, C. J. *Adv. Mater.* **2001**, *13*, 1389.
(16) Jana, N. R.; Gearheart, L.; Murphy, C. J. *Chem. Mater.* **2001**, *13*, 2313.
(17) Murphy, C. J.;.Jana, N. R. *Adv. Mater.* **2002**, *14*, 80.
(18) Jana, N. R.; Gearheart, L.; Obare, S. O.; Murphy, C. J. *Langmuir* **2002**, *18*, 922.
(19) Jana, N. R.; Gearheart, L.; Murphy, C. J. *J. Phys. Chem. B.* **2001**, *105*, 4065.
(20) Haynes, C. L.; McFarland, A. D.; Zhao, L. L.; Van Duyne, R. P.; Schatz, G. C.; Gunnarsson, L.; Prikulis, J.; Kasemo, B.; Kall, M. *J. Phys. Chem. B.* **2003**, *107*, 7337.
(21) Haynes, C. L.; Van Duyne, R. P. *Nano Lett.* **2003**, *3*, 939.
(22) Aslan, K.; Lakowicz, J. R.; Geddes, C. D. *J. Phys. Chem. B* **2005**, *109*, 3157.
(23) Taub, N.; Krichevski, O.; Markovich, G. *J. Phys. Chem. B* **2003**, *107*, 11579.
(24) Wei, Z.; Mieszawska, A. J.; Zamborini, F. P. *Langmuir* **2004**, *20*, 4322.
(25) Geddes, C. D.; Cao, H.; Gryczynski, I.; Gryczynski, Z.; Fang, J.; Lakowicz, J. R. *J. Phys. Chem. A* **2003**, *107*, 3443.
(26) Lakowicz, J. R. *Anal. Biochem.* **2001**, *298*, 1.
(27) Lakowicz, J. R.; Shen, Y.; D'Auria, S.; Malicka, J.; Fang, J.; Grcyzynski, Z.; Gryczynski, I. *Anal. Biochem.* **2002**, *301*, 261.
(28) Geddes, C. D.; Lakowicz, J. R. *J. Fluoresc.* **2002**, *12*, 121.
(29) Geddes, C. D.; Aslan, K.; Gyrczynski, I.; Malicka. J.; Lakowicz, J. R. *Rev. Fluoresc.* **2004**, *1*, 365 and references therein.
(30) Lakowicz, J. R.; Geddes, C. D.; Gryczynski, I.; Malicka, J.; Gryczynski, Z.; Aslan, K.; Lukomska, J.; Matveeva, E.; Zhang, J.; Badugu, R.; Huang, J. *J. Fluoresc.* **2004**, *14*, 425.
(31) Malicka, J.; Gryczynski, I.; Geddes, C. D.; Lakowicz, J. R. *J. Biomed. Opt.* **2003,** *8* (3), 472.
(32) Gryczynski, I.; Malicka, J.; Geddes, C. D.; Lakowicz, J. R. *J. Fluoresc.* **2003** *12*, 11.
(33) Geddes, C. D.; Parfenov, A.; Roll, D.; Fang, J.; Lakowicz, J. R. *Langmuir* **2003**, *19*, 6236.
(34) F Schutt, F.; Fischer, J.; Kopitz, J.; Holz, F. G. *Clin. Exp. Invest.* **2002**, *30*, 110.
(35) Sevick-Muraca E. M.; Lopez, G.; Reynolds, J. S.; Troy, T. L.; Hutchinson, C. L. *Photochem. Photobiol.* **1997**, *66*, 55.
(36) Sokolov, K.; Chumanov, G.; Cotton, T. M. *Anal. Chem.* **1998**, *70*, 3898−3905.
(37) Lakowicz, J. R. L. *Anal. Biochem.* **2005**, *337*, 171.
(38) Geddes, C. D.; Lakowicz, J. R. L. *J. Fluoresc.*, in press.